

**A novel nanosized layered double hydroxide ceramic based extended
release drug delivery system for cancer therapy**

Synopsis Submitted by,

Suman Saha

For the degree

of

Doctor of Philosophy (Pharmacy)

**Department of Pharmaceutical Technology
Jadavpur University
Kolkata, India
2022**

Self-Declaration

I, Suman Saha a PhD registered candidate of Jadavpur university having **enrolment No D-7/ISLM/69-16 dated 08.09.2016** do hereby declare that this Synopsis entitled **“A novel nanosized layered double hydroxide ceramic based extended release drug delivery system for cancer therapy”** contains original research work done by the undersigned candidate as part of doctoral studies.

All information in this synopsis have been obtained and presented in accordance with existing academic rules and ethical conduct.

Signature of the candidate

Prof.(Dr.) Tapan Kumar Chatterjee, (Supervisor)
Dean, Dept. of Pharmaceutical Science and Technology
JIS University, Kolkata
Former Professor, Division of Pharmacology
Former Director, Clinical Research Centre (CRC)
Jadavpur University
Kolkata-700032, India

Dr. Jui Chakraborty(Supervisor)
Principal Scientist
Bioceramics and Coating Div
CSIR-Central Glass and
Ceramic Research Institute
Kolkata-700032

CERTIFICATE FROM THE SUPERVISOR

This is to certify that the synopsis entitled “**A novel nanosized layered double hydroxide ceramic based extended release drug delivery system for cancer therapy**” submitted by Suman Saha, who got his name registered having enrolment No D-7/ISLM/69-16 dated 08.09.2016 for the award of Ph.D. (Pharmacy) degree of Jadavpur University is absolutely based upon his own work under the supervision of the undersigned and that neither this synopsis nor any part of it has been submitted for any degree/diploma or any other academic award anywhere before.

Signature & Seal

Prof (Dr.) T. K. Chatterjee
Dean,
Dept. of Pharm. Science and Tech.
JIS University, Kolkata
Former Professor, Division of Pharmacology
Former Director, Clinical Research Centre (CRC)
Jadavpur University
Kolkata-700032, India

Dr. Jui Chakraborty
Principal Scientist
CSIR-Central Glass &
Ceramic Research Institute
Jadavpur, Kolkata-700032
India

Table of Contents

| | Page No. |
|---|----------|
| 1. Background and Introduction | 1 |
| 2. Aims & Objectives of the present study | 6 |
| 2.1. The specific objective of the present study includes | 6 |
| 3. Experimental Procedures | 8 |
| 3.1 Synthesis of pristine bare CaAl-LDH at three pH conditions | 8 |
| 3.2 Synthesis of the etoposide (ETO) loaded CaAl-LDH nanoparticle (sample B) by anion exchange technique..... | 8 |
| 4. Significant Results and Discussion | 10 |
| 4.1. PXRD analysis of CaAl-LDH..... | 10 |
| 4.2. Morphological assessments of sample C (pH 12.5)..... | 11 |
| 4.3. TEM analysis of sample A (pH 8.5) and sample C (pH 12.5)..... | 12 |
| 4.4. <i>In vitro</i> Cell viability study of all the samples (A, B and C)..... | 12 |
| 4.5. PXRD analysis sample A (phase pure CaAl-LDH) and sample B (ETO incorporated CaAl-LDH)..... | 15 |
| 4.6. <i>In vitro</i> drug release kinetics from sample B and physical mixture..... | 15 |
| 4.7. <i>In vitro</i> cell viability and cell migration assay of ETO, sample A and B..... | 17 |
| 4.8. <i>Cellular</i> uptake study of Sample B into A549 cell line..... | 19 |
| 4.9. Cellular internalization of sample B in A549 cell line..... | 20 |
| 5. Conclusion | 21 |
| 6. References | 22 |

1. Background and Introduction

Cancer is one of the most important serious health issues and is the second common factor associated with death worldwide. However, pathogenesis of cancer is diverse and most of the time is associated with physicochemical and biological occurrence. In cancer there is a series of abnormal mutations in the genetic code which leads to uncontrolled cell growth. Therefore, the function of the cells are hampered, and abnormalities are noted (Saha et al., 2016). In case of cancer prognosis, the proto-oncogenes are held responsible for cell division and growth under normal condition though in some special occasions during the mutation phase these oncogenes mutate abnormally and becomes dangerous.

Although there are hundreds of cancer type and all are different in each other in all aspect including pathogenesis involved, prognosis, treatment strategies, life expectancy and many more, however regular screening, high risk patient with significant family history, early diagnosis have improved the patient prognosis and health outcome (Jang et al., 2003). It is evident that almost 80% of the cancers are solid tumours which can be surgically removed, prior to which chemotherapy and radiotherapy is the main choice of treatment for the reduction in tumour size and association of other organs at the tumour site (Jang et al., 2003). Moreover other treatment strategy includes immunotherapy/immunosuppression, gene and hormonal therapy, transplantation etc. (Leach, 1999). Chemotherapy predominates significantly owing to its lower adverse effect compared to other means of treatment however, there are several obstacles associated to killing of all the cancer cells and difficult to manage when the cells are metastasized to other organs of importance. There are several reasons that contribute to the failure of the chemotherapy in cancer treatment. The notable parameters including selectivity of inappropriate drugs/cycles, multi drug resistance, heterogenous

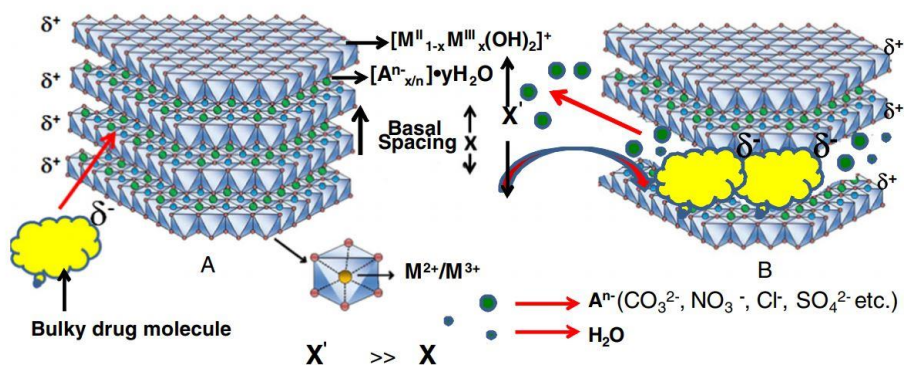
biological factors for cancer etc. Moreover, there are many other parameters associated with the drug itself including poor solubility at physiological pH, targeting of the drug to the site etc. Because of these factors, the present treatment strategy requires high dosage which can exhibit multitude of adverse events including nausea and vomiting, pain in muscle, hair loss, headaches, diarrhoea, appetite loss, throat scores, etc. resulting in lower patient compliance (Minchinton, and Tannock, 2006). Further most of the anticancer drugs are insoluble or have lower solubility in aqueous medium therefore for solubilization of the drug, various toxic chemical substances are in use which often exhibits several adverse events hence increase the morbidity and mortality rate (Feng, and Chien, 2003; Torchilin, 2004).

The major concern persists with the conventional chemotherapy related to the pharmacological and physicochemical properties of the drug molecule. Anticancer drugs delivered directly do not have the best therapeutic efficacy owing to several problems, including low absorption, enzymatic degradation, adverse drug reactions due to high dosage, and systemic toxicity due to local accumulation [Saha et al., 2016]. Further higher dosage of a drug is required in case of short plasma half-life which further leads to nonspecific toxicities to the proliferating cells. Therefore, it is of prior importance to choose an efficient and safe delivery system of anticancer drug. Therefore, nanoparticle mediated drug delivery is an important choice as it allows a controlled release of the moiety to the target site thereby reduced accumulation of drugs in the body that results in reduced toxic side effects and dosage frequency. When compared to typical bare pharmaceuticals, the employment of suitable nanoparticles (e.g., biocompatible and biodegradable) in drug delivery applications is a significant topic because of their small size, enhanced solubility which is expected to display maximal performance. Nano drug delivery is one of the most challenging approaches

towards the treatment of many diseases including cancer that helps to overcome several conventional drug delivery related drawbacks. As a result, in recent years, several nanoparticles, including as polymeric, liposomes, metal oxide, composites, and ceramics, have been extensively explored for the above-mentioned use (Hassan et al., 2020).

As the nanoparticle-based drug delivery is gaining popularity among the formulation scientists, both small and large drug molecules are under investigation for the treatment of cancer which has a significant potential to revolutionize the landscape of biopharmaceutical field.

In this regard, layered double hydroxide (LDHs), a type of ceramic material (anion exchanger clay substance), has long been utilised as a catalyst, ceramic precursor, and additive for polymers, among other things. Although the nanoscale production of materials has opened up a new arena in the field of drug/gene delivery with applications in nanomedicine (Choy et al., 2007). Moreover, their intrinsic extraordinary features including pH dependant degradability, high swelling property, ease of surface functionalization, tailor made anion exchange capacity and chemical inertness, it can be used as an excellent carrier of drug/biomolecule, genes, small interfering RNA (siRNA)/ other small molecules and thereby the controlled release property of the material makes it a suitable alternative to polymeric nanoparticle in the field of drug delivery (Kriven et al., 2004; Choi et al., 2009).



Scheme 1 Ion exchange allows the molecule to be inserted into the interlayer/interlamellar space of the bilayer via cationic layers of LDH (Saha et al., Appl. Clay Sci. 2016)

An anionic layered mineral (LDH) is composed of charge-balancing hydrated gallery anions and charged metal hydroxide layers. $[M^{II}_{1-x}M^{III}_x(OH)_2]^+[A^{n-}_{x/n}]^{\bullet}yH_2O$, in which M^{II} denotes bivalent metal ions such as Mg, Ca, Zn, Ni, Cu, Co, and M^{III} denotes trivalent metal ions such as Al, Cr, Fe, Ga, and so on. The ions are able to occupy octahedral core of brucite layers, e.g., $M^{II}-O-M^{III}-OH$, that forms positive layers which exhibits strong interaction between the layers and the electro neutrality of the structure is maintained by the presence of hydrated exchangeable anions. CO_3^{2-} , NO_3^- , Cl^- , SO_4^{2-} etc (Scheme 1), and x = molar ratio of $M^{II}/(M^{II}+M^{III})$ comes within the range of 0.25 - 0.33, yields LDH structure (either 2:1 or a 3:1) respectively. Moreover, function of the anion is denoted by y and the x/n term achieves charge neutrality throughout the LDH structure (Chakraborty et al., 2013).

Herein, Lung carcinoma is a malignant lung tumour marked by uncontrollable cell proliferation in the lungs. By metastasizing into neighbouring tissue or other sections of the body, this abnormal tissue growth might expand beyond the lung (Cooper GM et al., 2000). Coughing (including coughing up blood), shortness of breath, normal weight loss, and chest pains are the most prevalent symptoms of lung cancer (Cooper GM et

al., 2000). Although various therapeutic options for lung cancer exist, such as surgery, radiation therapy, chemotherapy, targeted therapy, and immunotherapy, the majority of them lack specificity and hence fail (Maeda et al., 2018). Though the side effects associated with the drug including schedule dependency and poor stability and less bioavailability often restricts it to exert the desired therapeutic action which leads to treatment failure. To overcome these drawbacks an attempt has been made to develop a novel (CaAl based) nanoceramic layered double hydroxide based extended-release drug delivery formulation encapsulating anticancer drug etoposide for the treatment of lung carcinoma.

2. Aims & Objectives of the present study

Etoposide been widely used as single or in combination as a first line drug in the treatment of lung cancer, though the side effects associated with the drug including schedule dependency and poor stability and less bioavailability often restricts it to exert the desired therapeutic action. To overcome these drawbacks an attempt has been made to develop a novel nanosized layered double hydroxide ceramic based extended-release drug delivery formulation encapsulating anticancer drug etoposide for the treatment of lung carcinoma.

2.1. The specific objective of the present study includes

1. The first objective was to synthesize a novel ceramic based CaAl-layered double hydroxides nanocarrier at varying pH condition and optimization of the same by different sophisticated analytical technique with extensive characterization (XRD, FTIR, FESEM, TEM, particle size, ion chromatography for carbonate estimation, in vitro cytotoxicity).
2. Second objective was to evaluate the anticancer potential of the synthesized nanocarriers at varying pH condition in colon cancer (HCT116), breast cancer (MCF7) and normal human osteoblast precursor (MC3T3) cell line. The motivation was to assess the optimized nanocarrier as a synergistic agent with the encapsulated drug molecule in cancer therapy.
3. The third objective was to encapsulate the drug etoposide in the optimized CaAl-LDH nanocarrier, extensive characterization followed by evaluating the synergistic anticancer potential of the nanoconjugate in lung cancer by cellular internalization of the nanoconjugate in the non-small cell lung carcinoma (A549) cell line.

The working hypothesis is that the etoposide encapsulated CaAl-LDH ceramic nanoparticles/nanohybrid formulation could have the potential anticancer property with reduced side effects and protects the healthy or normal tissues from the harmful toxicity of the bare drug.

3. Experimental Procedures

3.1 Synthesis of pristine bare CaAl-LDH at three pH conditions

CaAl-LDHs were effectively synthesized at varying pH condition 8.5, 10.5 and 12.5. Herein, 32 mmol of $[\text{Ca}(\text{NO}_3)_2 \cdot 4\text{H}_2\text{O}]$ and 16 mmol of $[\text{Al}(\text{NO}_3)_3 \cdot 9\text{H}_2\text{O}]$ in 250 ml of decarbonated water (18.2 M) and stirring continuously under a nitrogen gas stream (XL grade, 99.99 percent pure). To obtain a white gelatinous suspension, by dropwise addition of the pH of the resulting mixed metal solution was M NaOH, the pH was adjusted to 8.5, 10.5 and 12.5 respectively. Sample A was the end product (LDH powder) obtained at pH 8.5, sample B obtained at pH 10.5 and sample C obtained at pH 12.5 respectively. CaAl-LDHs were manufactured using the same process as before, but at pH values ranging from 8 to 13, with (pH 8.5, 10.5, and 12.5) serving as representative instances.

Extensive physicochemical characterizations (Powder X-ray diffraction (PXRD) of all the samples (A, B and C), Fourier transform infrared (FTIR), particle size and morphology, Assessment of trace level carbonate ion (ppm) in all the samples including purged water, *In vitro* dissolution study of Ca^{2+} ion in simulated body fluid (SBF), *In vitro* anticancer activity of the samples A, B and C) were undertaken for all the samples

3.2 Synthesis of the etoposide (ETO) loaded CaAl-LDH nanoparticle (sample B) by anion exchange technique

Etoposide (ETO) loaded CaAl-LDH nanoparticle Sample B was made using a basic anion exchange method (Qin et al., 2010). In a nutshell, around 50 ml of 0.1 M ETO solution was made by mixing ETO with Millipore water (pH was adjusted to 8 by dissolving NaOH pellet). Furthermore, under constant nitrogen purging, the ETO

solution was added to a 100 ml aqueous suspension of 1 g (equal to the equivalent quantity of nitrate ions) of sample A (CaAl LDH at pH 8.5) and thereafter drop by drop, 0.01 M NaOH was added until the pH was elevated to 10. The entire synthesis procedure was carried out while the reaction vessel was agitated for 48 hours. At 82 °C and 10 Pa pressure, the resultant suspension was centrifuged, washed, and freeze dried. Sample B is the name given to this sample (Qin et al., 2010).

Physicochemical characterizations (Powder X-ray diffraction (PXRD), Fourier transform infrared (FTIR), particle size and morphology, loading % of ETO, *in vitro* release of ETO from sample B, half maximal inhibitory concentration (IC₅₀) of ETO on A549 (lung adenocarcinoma) cell line, IC₅₀ of sample B on lung carcinoma cell line (A549), sample B's time-dependent synergistic activity in comparison to bare ETO and sample A, Cell proliferation/migration assay *invitro* using sample B, cellular internalization, CaMKII α expression, SOD assay) were undertaken.

4. Significant Results and Discussion

4.1. PXRD analysis of CaAl-LDH

The phase pure CaAl-LDH is confirmed by the basal spacing (d_{002}) of 8.66 Å, which corresponds to the (002) peak of CaAl-LDH (JCPDF 01-089-6723). The X'Pert PRO software was used to validate the phases. Sample B, produced a combined phase including both pure CaAl-LDH (63%) and CaCO₃ (aragonite and calcite polymorphs) (37%) (JCPDF 00-022-0147). While in sample C, the proportion of CaCO₃ was increased to 43%, with both aragonite and calcite polymorphs (CaAl-LDH (JCPDF 00001-0628 and 01072-1214 respectively).

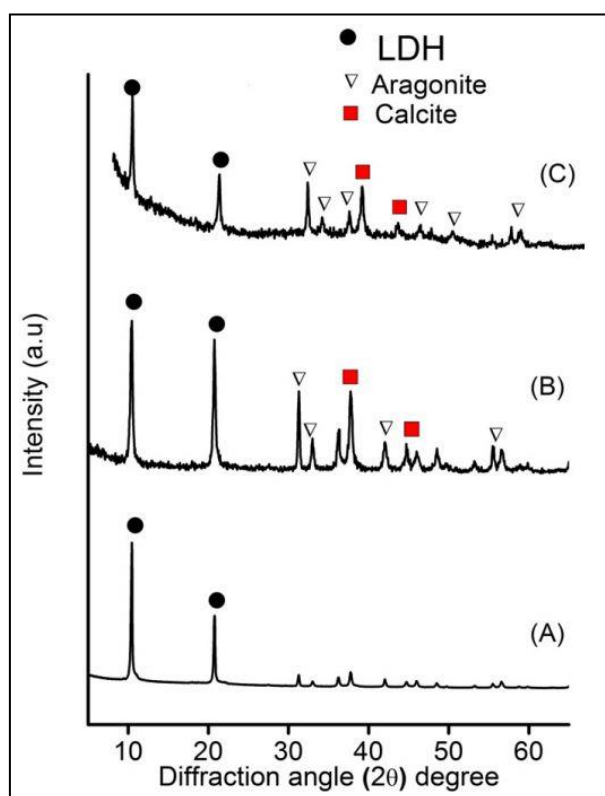


Figure 1. The XRD pattern of all the samples (A, B and C) exhibits phase pure and mixed phase containing LDH

4.2. Morphological assessments of sample C (pH 12.5)

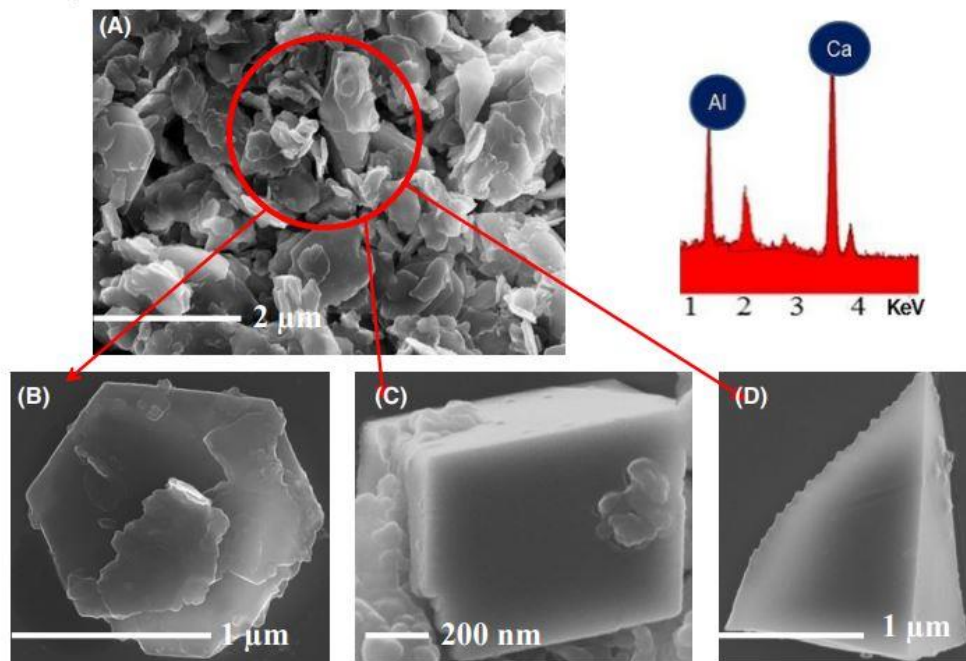


Figure 2. FESEM pictures of (A) sample C containing a mixture of CaAl-LDH (B) CaCO_3 (C calcite polymorph) and CaCO_3 (D aragonite polymorph). (E) EDS (A) of the respective area, with CaAl-LDH as the dominant phase.

2B, a hexagonal platelet is a typical characteristic of LDH usually (CaAl-LDH), A rhombohedron crystal at 2C illustrates the development of calcite polymorph, the most well-known and stable calcium carbonate polymorph. Intriguingly, the presence of the aragonite polymorph could be established in the same precipitated phase, as illustrated in 2D, a typical orthorhombic system with a prismatic crystal habit.

4.3 TEM analysis of sample A (pH 8.5) and sample C (pH 12.5)

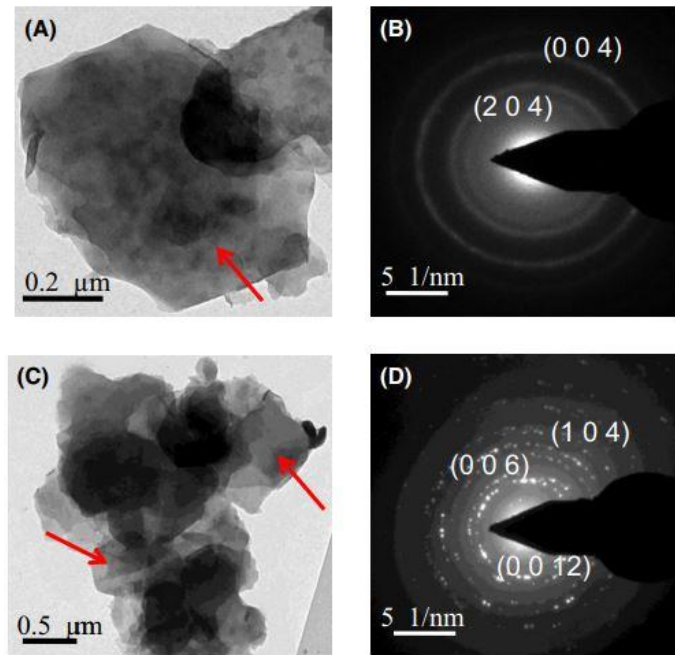


Figure 3. TEM images of sample A (A), where the arrow indicates hexagonal platelets (B). Sample C shows the distinctive atomic planes (C) sample C, where the arrow indicates the existence of calcite polymorph (D) sample C's SAED pattern.

TEM pictures confirm the presence of calcite crystals in sample C, as shown by FESEM and XRD data. The atomic planes that correspond to the layered clay structure of CaAl-LDH and CaCO_3 , as well as the XRD data, has been confirmed by the SAED image (Figure 3 B,D).

4.4. *In vitro* Cell viability study of all the samples (A, B and C)

All three samples (A, B, and C) were examined for cell viability at three different time points (24, 48, and 72 h) using colon and breast cancer cell lines (HCT116 and MCF7) and healthy bone cells (MC3T3) (osteoblast precursor). Part A shows a strong suppression of cell growth (HCT116) to 49.79 % in 24 h for sample A, which increases

to 57.64 % at 48 hours, and then to 70.77 percent at 72 hours [Figure 4, part A, panel (A)]. For sample A only, panel (B) exhibits a similar tendency (to a lesser extent of 39.38 % within 24 hours, followed by 43.62 % at 48 h, which increases to 46.80% at 72h respectively), However, utilising the cancer cells HCT116 and MCF7, no significant impacts were observed for samples B and C at the above-mentioned time intervals. MC3T3 cells have a high viability (95-98%) in the presence of all three samples A, B, and C, with no inhibitory effect on healthy cells. The significance of the data was determined at a confidence interval (CI) of 95 percent and a value of $P < 0.05$.

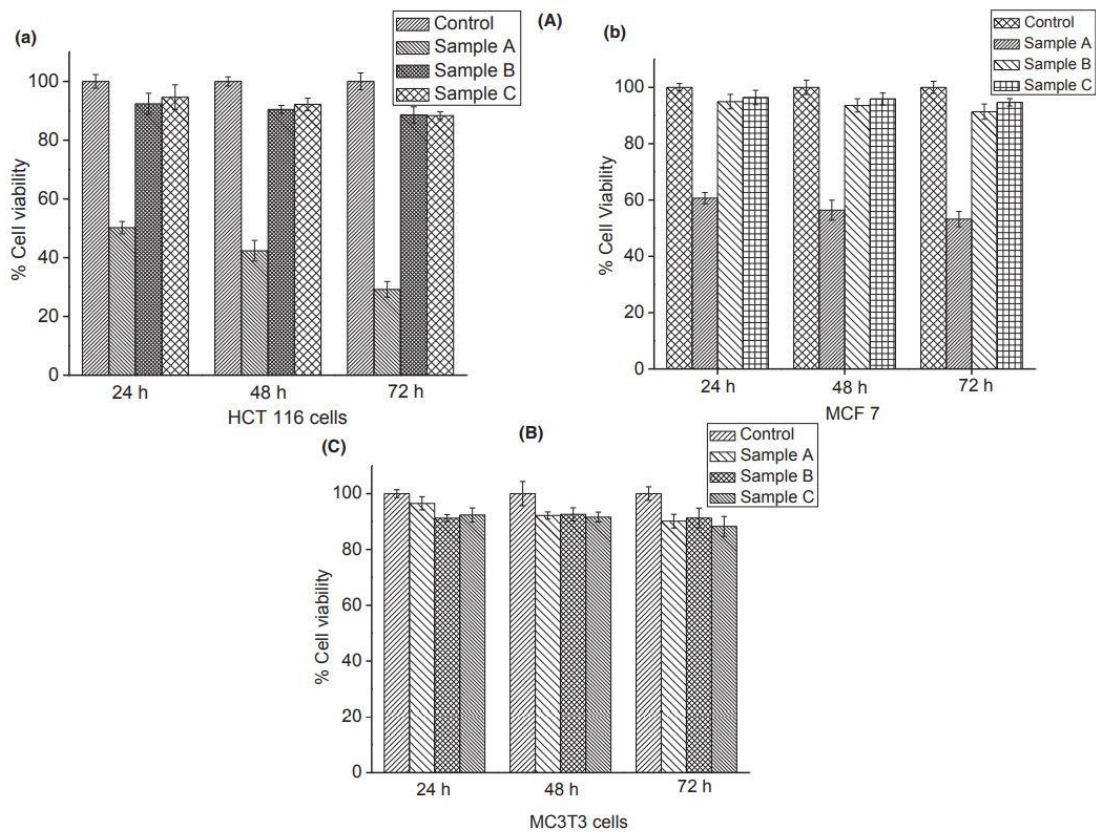


Figure 4. Part (A) uses samples A, B, and C to demonstrate the vitality of cancer cells (HCT 116 and MCF7). Part (B) shows the results as in the healthy cell line, MC3T3 osteoblast precursor.

In Sample B and sample C (CaAl-LDH at pH 10.5 and 12.5), both the polymorphs (calcite/aragonite) of CaCO₃ were precipitated, as well as phase pure CaAl-LDH. The calcium concentration of e.g., sample A (phase pure, 100 percent CaAl-LDH) > sample B (CaAl-LDH+CaCO₃) > sample C (CaAl-LDH+CaCO₃), determines the dissolution profile of Ca²⁺ at a certain time point (e.g., 24 hours). At pH more than 10, calcium ion creates hydroxide precipitates, and their solubility increases as pH decreases. Because the solubility product of calcium hydroxide K_{sp} is higher than that of the two crystalline polymorphs of calcium carbonate (aragonite) and (calcite), the dissolution of the Ca²⁺ ion from the hydroxide homologue is significantly greater than that of the carbonate salt. As a result, more Ca²⁺ is collected in the cells of sample A, increasing the cellular Ca²⁺ concentration and limiting cancer cell proliferation. In contrast to samples B and C, which have larger particle sizes, sample A (phase pure CaAl-LDH) has a smaller particle size, which allows it to pass into the cancer cell more easily, probably by an endocytosis mechanism. A significant statistical difference (P<0.05) was found in the in vitro cytotoxicity assay of sample A. Less calcium ion dissolution, which leads to less calcium ion accumulation in cancer cells (HCT116 and MCF7), which gradually reduces anticancer efficacy, as discussed above, based on intracellular calcium ion concentration and its influence on cancer cell apoptosis.

4.5. PXRD analysis sample A (phase pure CaAl-LDH) and sample B (ETO incorporated CaAl-LDH)

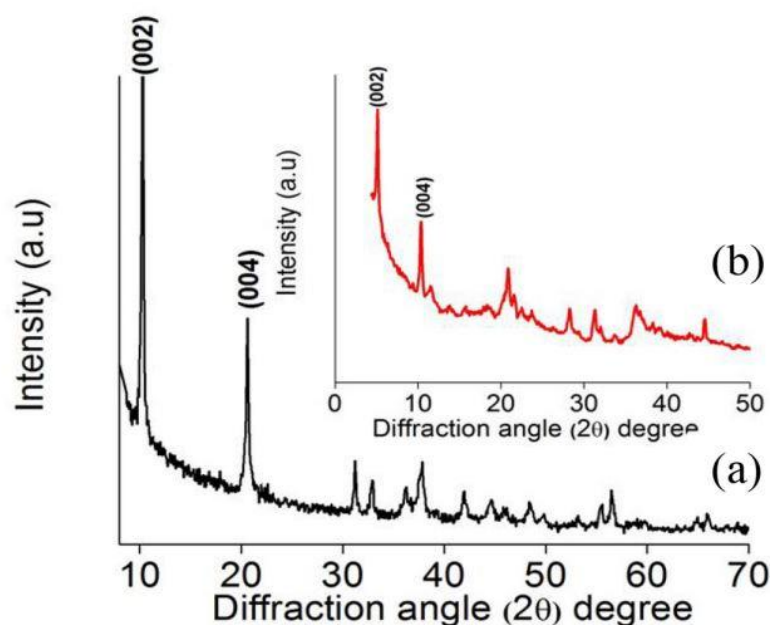


Figure 6. Powder X-ray diffraction patterns of (a) sample A (phase pure CaAl-LDH) (b) sample B (ETO incorporated CaAl-LDH).

Figure 6. shows the powder X-ray diffraction (XRD) patterns of samples A and B. As shown in Figure 6, the basal spacing (d_{002}) of 8.5764 corresponds to the (002) diffraction peak of sample A (JCPDF 01-089-6723), which rose to 17.18 in sample B as the corresponding peak (002) migrated from $2\theta = 10.31$ to $2\theta = 5.14$. This is owing to the enlargement of the interlayer space caused by the drug ETO being inserted into sample A along the z-axis, which represents the layer stacking direction in the nanoconjugate.

4.6. *In vitro* drug release kinetics from sample B and physical mixture

To suit the *in vitro* ETO release from sample B, different release kinetics models were used. The dialysis membrane diffusion technique was used to investigate the *in vitro*

ETO release from sample B and a physical mixing of the two (ETO and sample A) (Ray et al., 2015). Result suggested that due to the lack of drug and nanocarrier interaction in the physical mixture almost complete (99.5%) release in the former case, within 12 h whereas in case of nanohybrid, the cumulative release of ETO from sample B exhibits an initial burst release of nearly 40% from the within the first 2 h owing to the loosely bound drug on the surface of the nanoparticle. The leftover drug, intercalated within the nanoparticle's interlayer space, follows ETO's prolonged release for up to 72 hours, which could be due to ETO's slow diffusion from the interlayer space of sample B (Ray et al., 2015).

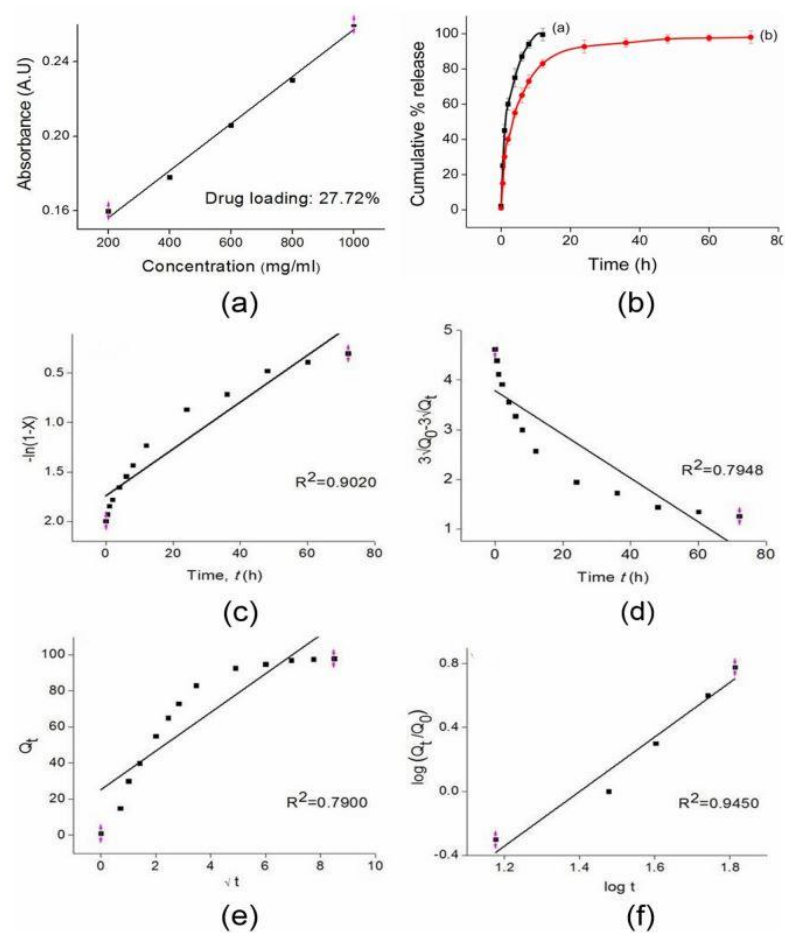
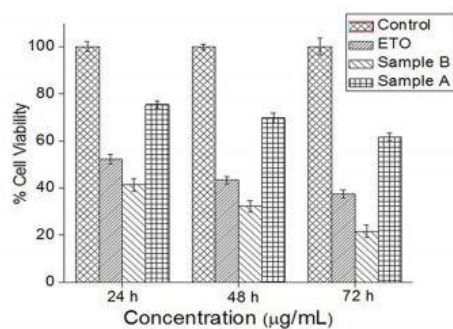


Figure. 7 (a) Calibration curve of etoposide gained from UV-VIS spectroscopy; (b) In vitro release of ETO from (a) Physical mixture of sample A and ETO (1:1, w/w) (b)

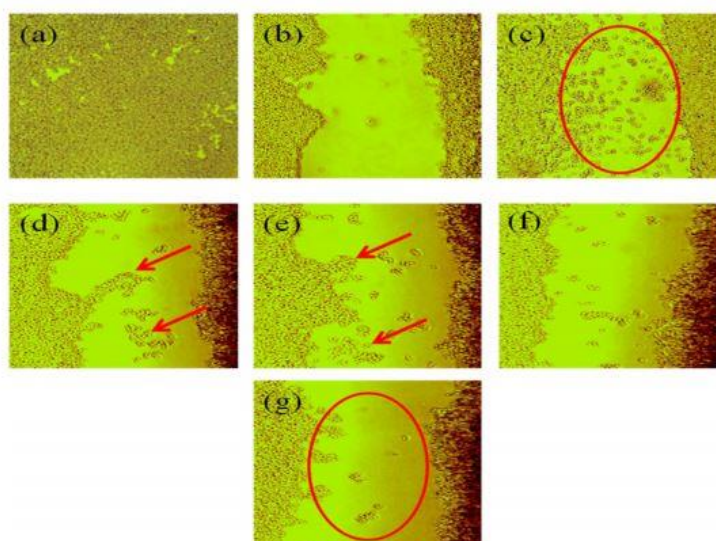
sample B in phosphate buffer saline at pH 7.4; (c)-(f) Release kinetics models (a) First-order model; (b) Hixon Crowel model; (c) Higuchi model (d) Korsmeyer-Peppas model.

Importantly, based on the obtained correlation coefficient (R^2) value 0.9450, the Korsmeyer-peppas model is proposed for the release of ETO from sample B. Furthermore, the kinetic exponent 'n' for sample B was 0.107, showing that the drug was released from the matrix in a regulated manner following a quasi-Fickian diffusion phenomena (Sahoo et al., 2012).

4.7. *In vitro* cell viability and cell migration assay of ETO, sample A and B



Part A



Part B

Figure 8. (A) In vitro cell viability study of the ETO, sample A and sample B on A549 cell line in varying time including 24, 48 and 72 h respectively; (B) In vitro cell migration assay shows (a) Confluent cells in 6 well plate (b) scratch by micropipette on the confluent plate (c) A549 cells without treatment (d) Cells treated with sample A (e) Cells treated with ETO (f) A549 cell treated with physical mixture (1:1, w/w) (g) Cells treated with Sample B

To test the synergistic anti-cancer potential of sample B, an in vitro cell viability investigation (Figure 8 A) was performed on the A549 cell line. Sample B's cell viability was reduced to 21.56 % after 72 hours when compared to bare ETO and sample A which showed a viability of 37.45 % and 61.85 %, respectively ($P < 0.05$). This is due to the cells' selectivity and the induction of mitochondrial apoptosis in cancer cells by disrupting the cellular membrane, that depends on ROS generation, which plays a crucial role in disrupting mitochondrial function and leading to apoptosis (Maiyo and Singh, 2017). Furthermore, the intracellular Ca^{2+} concentration is important in controlling the apoptotic pathway. This apoptotic mechanism backs up the previous findings (Saha et al., 2018). The proliferation/migration assay of the A549 cell line is shown in Figure 8 B after treatment with sample A, bare ETO, physical mixture of CaAl-LDH and ETO in (1:1 w/w ratio), and sample B. We found that sample A treated cells proliferate at 48.70 % compared to 59.34 % in control cells, indicating anti-cancer action similar to that previously reported by our study group (Bhattacharjee et al., 2019). Further, proliferation was much lower in sample B (18.62%) compared to bare ETO (37.89%), and physical mixture of CaAl-LDH and ETO in (1:1 w/w ratio) was 34.66 % ($P < 0.05$), indicating sample B's synergistic anticancer potential (ETO intercalated in sample A). Due to the failure to give the drug with a prolonged release effect from the nanoconjugate, the physical mixture did not show substantial

cytotoxicity when compared to Sample B. The synergistic anti-cancer potential of sample B (ETO intercalated CaAILDH) could be linked to the apoptotic pathway mechanism described above. The cellular absorption of sample B in the A549 cell line, which was expressed by Fluorescein isothiocyanate, was measured by flow cytometry (FITC).

4.8. Cellular uptake study of Sample B into A549 cell line

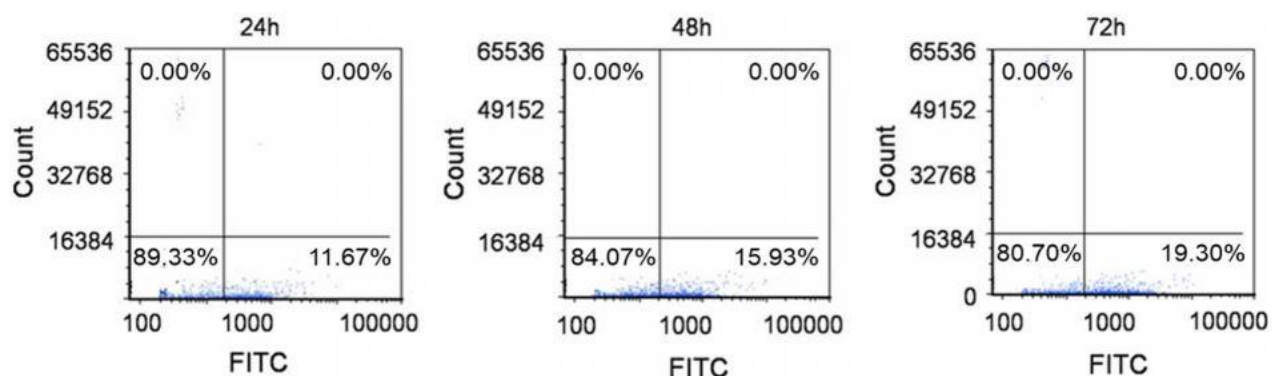


Figure 9 exhibits uptake of FITC tagged sample B into A549 cell line, showing internalization of the nanoconjugate into the cell (sample B);

Figure 9 shows conventional FACS profiles, which shows a strong uptake profile of sample B in a time-dependent manner. The cellular absorption was determined to be 11.67 % after 24 hours and rose to 19.30 % after 72 hours of incubation. This finding backs with evidence from an in vitro cytotoxicity study, which implies that sample B has a synergistic anti-cancer effect.

4.9. Cellular internalization of sample B in A549 cell line

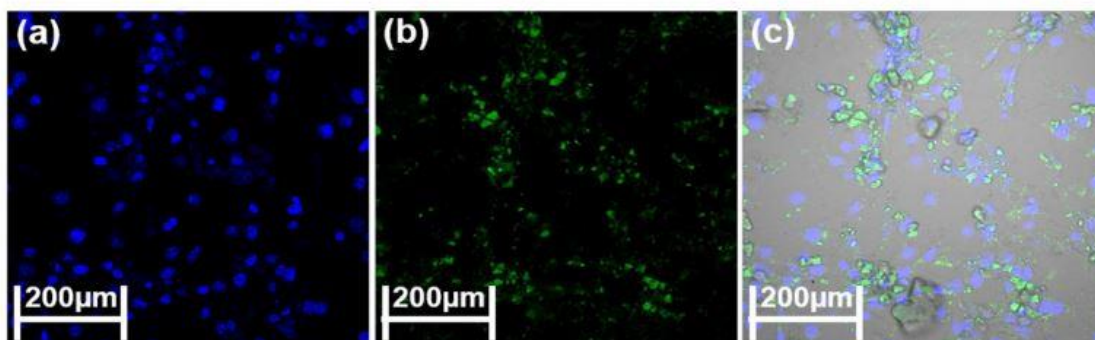


Figure 10. Confocal image of (a) DAPI image (b) FITC image (c) superimposed image.

Confocal laser scanning microscopy (CLSM) pictures, displayed in Figure 10, corresponding to 24 hours of incubation time, confirmed the above observation of cellular uptake of the FITC tagged sample B employing A549 cells. The presence of FITC-tagged sample B in the intracellular matrix indicated that sample B had successfully internalised the matrix, which was confirmed by nuclei stained by DAPI.

5. Conclusion

The study demonstrates a pH-dependent synthesis of CaAl-LDH by a straightforward coprecipitation approach technique (at pH 8.5, pH 10.5, and pH 12.5). Surprisingly, phase pure CaAl-LDH was generated at a lower pH 8.5 but an increase in pH results in the development of CaCO₃ (both aragonite and calcite polymorphs) (pH 10.5 and 12.5), as well as CaAl-LDH. Further the in vitro cytotoxicity study using human colon cancer cell line (HCT116) revealed growth suppression using sample A after 24 hours, which increased to 70.77 percent after 72 hours, showing substantial anticancer efficacy. Healthy bone cells (MC3T3) were used to confirm the findings, and all three samples showed good vitality (95-98%). In this part the present study opens a new avenue for using phase pure (100%) CaAl-LDH as an active anticancer agent.

Moreover, anti-cancer drug etoposide was intercalated into the phase pure LDH. When comparing the CaAl-LDH-ETO nanoconjugate (sample B) to bare CaAl-LDH (sample A) and the etoposide drug, the synergistic anti-cancer capability of the CaAl-LDH-ETO nanoconjugate (sample B) was discovered. Further the in vitro cell viability on A549 (human lung adenocarcinoma) cells showed considerable growth inhibition (21.56 percent in 72 hours) when sample B (ETO loaded nanoconjugate) was used, which was subsequently corroborated by cell proliferation/migration assay.

In conclusion, this study uncovers a novel element of synergism for etoposide a well-known anticancer drug and a suitable delivery carrier (phase pure CaAl-LDH) which provides a new route for its application in a more effective way in the management of lung carcinoma.

6. References

Bhattacharjee, A., Rahaman, S.H., Saha, S., Chakraborty, M., Chakraborty, J., 2019. Determination of half maximal inhibitory concentration of CaAl layered double hydroxide on cancer cells and its role in the apoptotic pathway. *Appl. Clay Sci.* 168, 31–35.

Chakraborty, J., Chakraborty, M., Ghosh, S., Mitra, M.K., 2013. Drug delivery using nanosized layered double hydroxide, an anionic clay. *Key Eng. Mater.* 571, 133–167.

Choi, S.J., Oh, J.M., Choy, J.H., 2009. Biocompatible ceramic nanocarrier for drug delivery with high efficiency. *J. Ceram. Soc. Jpn.* 117, 543-549.

Choy, J.H., Choi, S.J., Oh, J.M., Park, T., 2007. Clay minerals and layered double hydroxides for novel biological applications. *Appl. Clay Sci.* 36, 122-132.

Cooper GM. *The Cell: A Molecular Approach*. 2nd edition. Sunderland (MA): Sinauer Associates; 2000. *The Development and Causes of Cancer*. Available from: <https://www.ncbi.nlm.nih.gov/books/NBK9963/>

Hassan, Saad & Kamel, Ayman & Maher, Heba. (2020). Drug delivery systems between metal, liposome, and polymer-based nanomedicine: a review. *European Chemical Bulletin*. 9. 91-102.

Kriven, W.M., Kwak, S.Y., Wallig, M.A., 2004. Bio-resorbable nanoceramics for gene and drug delivery. *MRS Bulletin*. 29, 33–37. Maeda H, Khatami M. Analyses of repeated failures in cancer therapy for solid tumors: poor tumor-selective drug delivery, low therapeutic efficacy and unsustainable costs. *Clin Transl Med.* 2018 Mar 1;7(1):11.

Maeda H, Khatami M. Analyses of repeated failures in cancer therapy for solid tumors: poor tumor-selective drug delivery, low therapeutic efficacy and unsustainable costs. *Clin Transl Med.* 2018 Mar 1;7(1):11.

Maiyo, F., Singh, M., 2017. Selenium nanoparticles: potential in cancer gene and drug delivery. *Nanomedicine (London)* 12 (9), 1075–1089.

Qin, L., Wang, M., Zhu, R., You, S., Zhou, P., Wang, S., 2013. The in vitro sustained release profile and antitumor effect of etoposide-layered double hydroxide nanohybrids. *Int. J. Nanomedicine* 8, 2053–2064.

Qin, L., Xue, M., Wang, W., Zhu, R., Wang, S., Sun, J., Zhang, R., Sun, X., 2010. The in vitro and in vivo anti-tumor effect of layered double hydroxides nanoparticles as delivery for podophyllotoxin. *Int. J. Pharm.* 388 (1–2), 223–230.

Ray, S., Joy, M., Sa, B., Ghosh, S., Chakraborty, J., 2015. pH dependent chemical stability and release of methotrexate from a novel nanoceramic carrier. *RSC Adv.* 5, 39482–39494.

Saha, S., Ray, S., Ghosh, S., Chakraborty, J., 2018. pH-dependent facile synthesis of CaAl layered double hydroxides and its effect on the growth inhibition of cancer cells. *J. Am. Ceram. Soc.* 101, 3924–3935.

Sahoo, S., Chakraborti, C.K., Behera, P.K., 2012. Development and evaluation of astrotentive controlled release polymeric suspensions containing ciprofloxacin and carbopol polymers. *J. Chem. Pharm. Res.* 4, 2268–2284.

List of publication in peer reviewed journals

1. **Saha S**, Ray S, Acharya R, Chatterjee T K, Chakraborty J. Magnesium, zinc and calcium aluminium layered double hydroxide-drug nanohybrids: a comprehensive study. **Applied Clay Science. (Elsevier)**. 2017, 135, 493-509. (SCI Impact Factor **3.64**).
2. **Saha S**, Ray S, Ghosh SK, Chakraborty J, pH-dependent facile synthesis of CaAl-layered double hydroxides and its effect on the growth inhibition of cancer cells, **Journal of the American Ceramic Society, Wiley publication**, 2018, 101(9), 3924-3935. (SCI Impact Factor **2.96**).
3. **Saha S**, Bhattacharjee A, Rahaman Sk H, Basu A, Chakraborty J, Synergistic anti metastatic activity of etoposide loaded calcium aluminium layered double hydroxide nanoconjugate in the management of non small cell lung carcinoma, **Applied Clay Science (Elsevier)**, 2020, **188, 105496** (SCI Impact Factor **3.64**).
4. **Saha S**, Bhattacharjee A, Rahaman H Sk, Ray S, Marei M K., Jain H , Chakraborty J, Prospects of antibacterial bioactive glass nanofibres for wound healing: an in vitro study. International Journal of Applied Glass Science. **Wiley publication, (Accepted, doi: 11.1111/ijag.15029)** (SCI Impact Factor **1.85**).
5. Ray S, **Saha S**, Sa B, Chakraborty J. *In vivo* pharmacological evaluation and efficacy study of methotrexate-encapsulated polymer coated layered double hydroxide nanoparticles for possible treatment of osteosarcoma. **Journal of Drug Delivery and Translational Research (Springer)**. 2017, 7(2), 259-275. (SCI Impact Factor **3.39**).
6. Acharya R, **Saha S**, Ray S, Hazra S, Mitra M K, Chakraborty J. siRNA-nanoparticle conjugate in gene silencing: A future cure to deadly diseases? **Materials Science and Engineering C (Elsevier)** 2017, 76 1378–1400 (SCI Impact Factor **5.08**)

7. Rahaman Sk. H, Bhattacharjee A, **Saha S**, Chakraborty M, Chakraborty J, shRNA intercalation in CaAl-LDH nanoparticle synthesized at two different pH conditions and its comparative evaluation, **Applied Clay Science. (Elsevier)**. 2017, 135, 493-509. (SCI Impact Factor **3.64**)
8. Bhattacharjee A, Rahaman Sk. H, **Saha S**, Chakraborty M, Chakraborty J, Determination of half maximal inhibitory concentration of CaAl layered double hydroxide on cancer cells and its role in the apoptotic pathway, **Applied Clay Science. (Elsevier)**. 2019, 171, 57-64. (SCI Impact Factor **3.64**)

Book chapter

1. **Suman Saha**, Payal Roy and Jui Chakraborty, Mesoporous silica-biopolymer based systems in drug delivery applications, Tailor-Made and Functionalized Biopolymer Systems, Elsevier, ISBN 978-0-12-821437-4, DOI: <https://doi.org/10.1016/B978-0-12-821437-4.00002-5>.
2. Acharya R, **Saha S**, Ray S, Chakraborty J, Nanoparticulate Immunotherapy: an intelligent way to tailor makes our defense system. Jana S and Jana S (Eds) Particulate Technology for Delivery of Therapeutics. Springer Nature Publication, New York, USA, ISBN 978-981-10-3646-0, 393642_1_En, (13) 2017, 419-451.

List of Patent

1. An inorganic base antacid compound with improved and novel properties, authored by Jui Chakraborty, Sayantan Ray, **Suman Saha**, Biswanath Sa, The Indian patent application number 0097NF2017, Docket no. 37407. CBR. No. 20680, Patent office application no. 201711020405, dated 12/06/2017.
(Indian) (Granted)
2. Bioactive glass particles and micro nano fibre based wound care compositions dressing, suture and matrices thereof, Jui Chakraborty, Suman Saha, Payal Roy, Rupam Saha, Application No: 202111046618, dated 12.10.2021. Council for Scientific and Industrial Research (Filed)
3. New compositions of bioactive glass based hemostatic matrices and preparation thereof, Puja Srivastava, Jui Chakraborty, Payal Roy, Suman Saha, Rupam Saha, Defence Research and Development Organization (Filed)

List of Presentations in National/International/Conferences/Workshops :

1. Saha S, Participated in “First International Conference on Emerging Materials: Characterization & Application” held on December 4-6, 2014 at CSIR- Central Glass and Ceramic Research Institute, Kolkata, India.

2. Saha S, Ray S, Joy M, Chakraborty J, “A layered nanocarrier in anticancer drug delivery path to a new horizon” in 6th East zonal & 24th state conference of Indian Pharmacological Society, WB branch, February 5- 6, 2015, West Bengal University of Animal and Fishery Sciences, Kolkata, India.

3. Saha S, Ray S, Chakraborty J, “CSIR-CGCRI developed novel inorganic based antacid: efficacy and toxicity study” in International Conference on Biomaterials, Biodiagnostics, Tissue Engineering, Drug Delivery and Regenerative Medicine 2016, held on April 15-17, 2016 at Indian Institute of Technology Delhi.

4. Saha S, Ray S, Chakraborty J, “A unique mouth melting inorganic antacid developed at CSIR-CGCRI for the treatment of hyperchlorhydria”, at the International Conference on Biotechnology and Biological Sciences (Biospectrum 2017), during August 25-26, 2017, held at University of Engineering and Management, Kolkata, India.

5. Saha S, Bhattacharjee A, Rahaman Sk H, Basu A, Chakraborty J, Synergistic anti metastatic activity of etoposide-CaAl layered double hydroxide nanoconjugate: A novel treatment approach for non small cell lung carcinoma, on Current Trends in Materials Science and Engineering 2019 on 18th-20th July 2019, held at S. N. Bose National Centre For Basic Sciences, Kolkata

6. Ray S, Saha S, Acharya R, Chakraborty J, “Value added multifunctional injectable bone augmentation material for treatment of osteoporotic vertebral compression

fracture in elderly patients” in International Conference on Energy, Functional Materials and Nanotechnology 2016 held on March 27-29, 2016 at Nanotechnology Center, Kumaun University, Nainital, India.

7. Ray S, **Saha S**, Acharya R, Sa B, Chakraborty J, “Unique bioactive glass based bone augmentation material for treatment of geriatric population suffering from osteoporotic vertebral compression fracture”, at the International conference on advances in glass science and technology held on January 23-25, 2017 at CSIR-Central Glass & Ceramic Research Institute.

Awards

1. Young Scientist Award from Material Research Society of India (MRSI), held at Indian Association for the cultivation of Sciences, Kolkata-700032 on 21.08.2018.

2. Best Oral Award at International Conference on Current Trends in Materials Science and Engineering 2019 on 18th-20th July 2019, held at S. N. Bose National Centre For Basic Sciences, Kolkata

3. Excellence in Research work Award at 2nd National Biomedical Research Competition, NBRCOM 2019 organized by Postgraduate Medical Education & Research, Chandigarh and Society of Young Biomedical Scientists (SYBS), India. Dated 17th November 2019.

4. Best Oral Presentation Award at International Conference on Synthesis, Characterization and Application of Nanomaterials (SCAN) organized by The Institution of Engineers (India), Dated 1-2 November 2019, Kolkata.